Science and Technology

RMUTT Journal

Vol.8 No.2 (2018): 53-64

www.sci.rmutt.ac.th/stj

Online ISSN2229-1547

DFT investigation of O_2 and PH_3 adsorptions on group 8B metal–doped boron nitride nanotubes

Ployvadee Sripadung[1], Nadtanet Nunthaboot[1,2] and Banchob Wanno[1,2,*]

[1] Supramolecular Chemistry Research Unit and Department of Chemistry, Faculty of Science, Mahasarakham University, Maha Sarakham, 44150, Thailand

[2] Center of Excellence for Innovation in Chemistry (PERCH–CIC), Faculty of Science, Mahasarakham University, Maha Sarakham, 44150, Thailand

*E–mail: banchobw@gmail.com

Abstract

The adsorptions of O_2 and PH_3 molecules on boron nitride nanotube (BNNT) with and without the doping of group 8B metals (TM) i.e. Fe, Ru, Os, Co, Rh, Ir, Ni, Pd, and Pt were investigated using a density functional theory calculation at the B3LYP/LanL2DZ theoretical level. The structural and electronic properties and adsorption abilities for the most stable configuration of gas adsorption on pristine and TM–doped BNNTs were calculated. The results indicate that the O_2 and PH_3 molecules show much stronger adsorption on the TM–doped BNNTs than that on the pristine BNNT. From our calculations, it is clearly imply that pristine BNNT is not suitable for gas sensing, while the Os_B–BNNT displays the highest interaction for O_2 adsorption and the Pt_B–BNNT displays the highest interaction for PH_3 adsorption. The electronic properties such as the energy gap, partial charge transfer, and density of state of TM–doped BNNTs are significantly modified after adsorptions. In conclusion, the TM–doped BNNTs can be used as O_2 and PH_3 gas storage and sensing in manufacturing raw materials.

Keywords: Adsorption, Boron nitride nanotube, DFT, Transition metal

Received: August 28, 2018

Revised: December 18, 2018

Accepted: December 21, 2018

1. Introduction

Boron nitride nanotubes (BNNTs) were successful synthesized in 1995 by Chopra and co–workers [1]. The BNNTs are wide band gap semiconductors. In additions, BNNTs have many unique properties such as chemical inertness, high thermal conductivity, high oxidation resistivity, and high tensile strength. These outstanding mechanical and chemical properties make BNNT useful in many fields such as gas storage, catalyst, biosensor and molecular adsorptions [2–3]. As an effective approach to improve the properties of BNNTs, doping impurity atoms into these nanostructures have been suggested. The structural and electronic properties of CO and NO molecules adsorbed on TM–(8,0) BNNTs (TM = V, Cr, Mn, Fe, Co, and Ni) were investigated, and the results show that the TM–doped BNNT could be used for as CO and NO gas sensors [4]. The adsorptions of small gases such as CO [5], NO_2 [6], and SO_2 [6] on metal–doped BNNTs were widely studied in theoretical theory for gas sensing applications. The adsorption and reactivity of O_2 on perfect and defective (10,0) BNNT were investigated using the density–functional theory (DFT) by Chen and his team. The results indicate that O_2 prefers to physically adsorb on perfect BNNT [7]. The DFT was used to predict oxygen adsorption on two types of hybrid carbon and boron–nitride nanotubes (CBNNTs), zigzag (8,0), and armchair (6,6), it is found that the O_2 adsorption is able to increase the conductivity of CBNNTs [8]. Phosphine (PH_3) is a by–product of sodium hypophosphite industry, colourless, and flammable. It is a high toxic waste gas for human acting on the central nervous system and lungs, leading to pulmonary oedema. Then, exposure of human beings even to small amounts should be avoided [9–11]. Previous works report that the adsorption of PH_3 affects the electronic properties of boron nitride nanoribbons [12] and zinc sulfide nanotubes [13]. Effective methods have been highly required to detect PH_3 gas for atmospheric environmental measurement and control. In the present work, adsorption abilities of O_2 and PH_3 gases on pristine and TM–doped BNNTs have been investigated using the DFT method. Electronic properties for all adsorption complexes of gas adsorptions on pristine and TM–doped BNNTs have been determined and their structures have been reported.

2. Computational details

The adsorptions of O_2 and PH_3 on pristine (5,5) armchair BNNT and its doping with group 8B TM atoms (Fe, Ru, Os, Co, Rh, Ir, Ni, Pd, and Pt) were investigated in terms of geometric and electronic properties in which both ends of all nanotubes were saturated by hydrogen atoms to avoid the boundary effects. Then the doping of TM atom onto the BNNT (TM–BNNT) was modeled so that one of boron or nitrogen atom at the middle site of the BNNT was replaced by the group 8B TM atoms. In this work, replacing of B or N atom of the BNNT with TM atom was referred to be the B (TM_B–BNNT) or N (TM_N–BNNT) sites, respectively. The adsorbed O_2 and PH_3 gases were

set by placing these molecules over the TM atom. All calculations were performed using the GAUSSIAN 09 software package [14] at the level of DFT with the Lee–Yang–Parr correlation functional (B3LYP) [15–17] and the intensive Los Alamos LanL2DZ split–valence basis set [19–20]. The B3LYP/LanL2DZ was employed because this standard method and basis set was successfully used for many studied systems of TM doping [21–26]. The spin multiplicity of each system is given in Table 1. The partial charge transfer (PCT) during gas adsorptions were defined as a change in gas charge between the adsorption processes using the natural bond orbital analysis. The molecular graphics of all optimized structures were generated using the MOLEKEL 4.3 program [27]. The electronic densities of states (DOS) of all systems were computed and plotted by the GaussSum 2.1.4 program [28]. The adsorption energies (E_{ads}) of O_2 and PH_3 molecules on the pristine and TM–doped BNNTs were determined through the following equation:

$$E_{ads} = E_{gas/\,BNNT} - (E_{BNNT} + E_{gas})$$

where $E_{gas/BNNT}$ was the total energy of O_2 or PH_3 adsorbed on pristine or TM–doped BNNT. E_{BNNT} was the total energy of the pristine or TM–doped BNNT, and E_{gas} was the total energy of the isolated O_2 or PH_3 molecule. A negative E_{ads} was referred to exothermic process.

3. Results and discussion

3.1 Geometrical structures of pristine and TM–doped BNNTs and their gas adsorptions

The geometrical structures of the O_2 and PH_3 adsorbed on pristine and TM–doped BNNTs were investigated. The optimized structures of the O_2 and PH_3 adsorbed on pristine BNNT are displayed in Fig. 1. The calculated binding distances (BD) between O_2 or PH_3 gas and pristine BNNT are 2.630 and 3.838 Å, respectively. The large BD values specify that the gases displayed weak adsorption on the BNNT pristine. This result is in accordance to the previous studies of the adsorptions of O_2 on single–walled boron nitride nanotubes [7] and PH_3 on boron nitride nanoribbons [12].

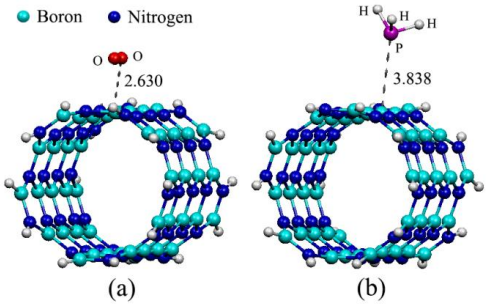

Figure 1 The optimized structures of (a) O_2 and (b) PH_3 adsorbed on pristine BNNT. The boron, nitrogen, oxygen, phosphorus, and hydrogen atoms are presented in cyan, blue, red, pink, and white balls, respectively. Bond distance is in Å.

The optimized structures of the O_2 and PH_3 adsorbed on TM–doped BNNTs are displayed in Figures 2 and 3, respectively. The protrusion on the surface of the TM–doped BNNTs is attributed to the larger atomic radius of TM atom relative to that of the B or N atom, the same trends can be found in the other works [4–5]. Our calculations produce the BDs between the adsorbed gas and TM atom, which are in the range of 1.712–2.248 Å for O_2 adsorption and 2.339–2.609 Å for PH_3 adsorption. The short BDs confirmed that the both gases show stronger adsorption with TM–doped BNNTs than that of pristine BNNT. These results are in good agreement with the previous works [4–6].

3.2 Adsorption energies of O_2 and PH_3 molecules adsorbed on pristine and TM–doped BNNTs

The adsorption energies of the O_2 and PH_3 on the pristine and TM–doped BNNTs are listed in Table 1. The absorption energies of the O_2 and PH_3 on the pristine are -6.60 and -1.32 kcal/mol, respectively. These indicate that the pristine BNNT displays weak sensitivity to the adsorption. The adsorption abilities of the O_2 adsorbed on the TM_B–BNNTs are in the order: O_2/Os_B–BNNT (-95.48 kcal/mol) > O_2/Ir_B–BNNT (-71.14 kcal/mol) > O_2/Ru_B–BNNT (–70.49 kcal/mol) > O_2/Pt_B–BNNT (-65.90 kcal/mol) > O_2/Fe_B–BNNT (-59.56 kcal/mol) > O_2/Pd_B–BNNT (-52.51 kcal/mol) > O_2/Ni_B–BNNT (–48.33 kcal/mol) > O_2/Rh_B–BNNT (-45.04 kcal/mol) > O_2/Co_B–BNNT (-33.72 kcal/mol). The adsorption abilities of the O_2 adsorbed on the TM_N–BNNTs are in the order: O_2/Pd_N–BNNT (–89.97 kcal/mol) > O_2/Pt_N–BNNT (-88.93 kcal/mol) > O_2/Ni_N–BNNT (-86.27 kcal/mol) > O_2/Os_N–BNNT (-81.26 kcal/mol) > O_2/Fe_N–BNNT (–80.79 kcal/mol) > O_2/Ru_N–BNNT (-71.49 kcal/mol) > O_2/Co_N–BNNT (-51.36 kcal/mol) > O_2/Rh_N–BNNT (-41.13 kcal/mol) > O_2/Ir–BNNT (-36.75 kcal/mol). The results show that the O_2 adsorptions on the TM–doped BNNTs are stronger than the pristine BNNT, in which Os_B–BNNT displays the strongest interaction with the O_2 molecule. The adsorption abilities of the PH_3 adsorbed on the TM_B–BNNTs are in the order: PH_3/Pt_B–BNNT (-23.47 kcal/mol) > PH_3/Os_B–BNNT (-22.78 kcal/mol) > PH_3/Ir_B–BNNT (-21.89 kcal/mol) > PH_3/Pd_B–BNNT (-17.68 kcal/mol) > PH_3/Ru_B–BNNT (–17.43 kcal/mol) > PH_3/Rh_B–BNNT (-17.04 kcal/mol) > PH_3/Fe_B–BNNT (-16.83 kcal/mol) > PH_3/Ni_B–BNNT (-15.70 kcal/mol) > PH_3/Co_B–BNNT (-12.78 kcal/mol). The adsorption abilities of the PH_3 adsorbed on the TM_N–BNNTs are in the order: PH_3/Fe_N–BNNT (-22.06 kcal/mol) > PH_3/Co_N–BNNT (-21.93 kcal/mol) > PH_3/Os_N–BNNT (-21.44 kcal/mol) > PH_3/Ni_N–BNNT (-21.03 kcal/mol) > PH_3/Ir_N–BNNT (-19.41 kcal/mol) > PH_3/Pd_N–BNNT (-16.29 kcal/mol) > PH_3/Ru_N–BNNT (-15.60 kcal/mol) > PH_3/Pt_N–BNNT (-15.41 kcal/mol) > PH_3/Rh_N–BNNT (-15.29 kcal/mol). The results show that PH_3 adsorptions on TM–doped BNNTs are stronger than pristine BNNT in which the Pt_B–BNNT displays the strongest interaction. Thus, the TM–doped BNNTs

are suitable for O_2 and PH_3 storage. It is worth to mention that the adsorption strengths of O_2 and PH_3 at TM_B– BNNTs are clearly consistent with the atomic radius i.e. Os > Ru > Fe and Pt > Pd > Ni, respectively. However, no correlation was obtained in the case of gas adsorption at the TM_N–BNNTs. In addition, for atoms from the same period (row), for instance, Fe, Co, and Ni, the correlation between adsorption energies and atomic radius was also not detected. This is possibly because the atomic radii of Fe, Co, and Ni are not significantly different in comparison with the case of atoms from the same group (column) such as Os, Ru, and Fe [29–30].

3.3 Electronic properties of pristine and TM–doped BNNTs and their gas adsorptions

The electronic properties of pristine and TM–doped BNNTs and their gas adsorptions in terms of energy gap (E_{gap}), and partial charge transfers (PCT) computed at B3LYP/LanL2DZ theoretical level are listed in Table 1. The results indicate that the E_{gap} of the pristine BNNT is computed to be 6.014 eV, which is in good agreement with the previous

Table 1 Adsorption energies (E_{ads}), energy gaps (E_{gap}), charge of energy gaps (ΔE_{gap}), partial charge transfers (PCT), and spin multiplicities (SM) of O_2 and PH_3 adsorbed on pristine and TM–doped BNNTs

Configurations	E_{ads} [a]	E_{gap} [b]	ΔE_{gap} [b,c]	PCT [d]	SM
O_2/BNNT	–6.60	2.041	–3.973	–0.098	1
O_2/Fe_B–BNNT	–59.56	2.395	–0.925	–0.231	2
O_2/Ru_B–BNNT	–70.49	2.259	0.028	–0.319	2
O_2/Os_B–BNNT	–95.48	2.068	–1.415	–0.582	2
O_2/Co_B–BNNT	–33.72	2.095	–1.361	–0.361	1
O_2/Rh_B–BNNT	–45.04	2.449	–0.952	–0.465	1
O_2/Ir_B–BNNT	–71.14	2.122	–1.252	–0.586	1
O_2/Ni_B–BNNT	–48.33	1.388	–0.381	–0.219	2
O_2/Pd_B–BNNT	–52.51	1.578	–0.327	–0.319	2
O_2/Pt_B–BNNT	–65.90	2.177	0.299	–0.416	2
O_2/Fe_N–BNNT	–80.79	2.748	–0.164	–0.472	2
O_2/Ru_N–BNNT	–71.49	2.857	–0.163	–0.310	2
O_2/Os_N–BNNT	–81.26	2.612	–0.082	–0.469	2
O_2/Co_N–BNNT	–51.36	2.177	–1.796	–0.371	1
O_2/Rh_N–BNNT	–41.13	1.415	–2.993	–0.507	1
O_2/Ir_N–BNNT	–36.75	2.122	–1.960	–0.403	1
O_2/Ni_N–BNNT	–86.27	2.367	0.245	–0.531	2
O_2/Pd_N–BNNT	–89.97	3.211	1.578	–0.520	2
O_2/Pt_N–BNNT	–88.93	3.238	1.524	–0.519	2
PH_3/BNNT	–1.32	6.014	0.000	0.019	1
PH_3/Fe_B–BNNT	–16.83	3.565	0.245	0.283	2
PH_3/Ru_B–BNNT	–17.43	2.286	0.055	0.296	2
PH_3/Os_B–BNNT	–22.78	2.177	0.109	0.342	2
PH_3/Co_B–BNNT	–12.78	3.429	–0.027	0.295	1
PH_3/Rh_B–BNNT	–17.04	3.184	–0.217	0.314	1
PH_3/Ir_B–BNNT	–21.89	2.993	–0.381	0.377	1
PH_3/Ni_B–BNNT	–15.70	3.238	1.469	0.327	2
PH_3/Pd_B–BNNT	–17.68	2.259	0.354	0.334	2
PH_3/Pt_B–BNNT	–23.47	2.150	0.272	0.400	2
PH_3/Fe_N–BNNT	–22.06	3.238	0.326	0.286	2
PH_3/Ru_N–BNNT	–15.60	2.993	–0.027	0.233	2
PH_3/Os_N–BNNT	–21.44	2.830	0.136	0.544	2

PH_3/Co_N–BNNT	–21.93	4.327	0.354	0.313	1
PH_3/Rh_N–BNNT	–15.29	4.708	0.300	0.246	1
PH_3/Ir_N–BNNT	–19.41	4.354	0.272	0.280	1
PH_3/Ni_N–BNNT	–21.03	1.986	–0.136	0.270	2
PH_3/Pd_N–BNNT	–16.29	1.687	0.054	0.207	2
PH_3/Pt_N–BNNT	–15.41	1.660	–0.054	0.235	2

[a] In kcal/mol

[b] In eV

[c] ΔE_{gap} defined as E_{gap}(gas/TM–BNNT) – E_{gap}(TM–BNNT)

[d] In *e*

[e] SM is the spin multiplicity.

measured [31] and calculated values [5]. When gases adsorbed on the pristine BNNT, the energy gap of the O_2 adsorption is changed while that of PH_3 does not. The energy gaps of the O_2/TM–BNNTs and PH_3/TM–BNNTs are found in the range of 1.388–3.238 and 1.660–4.708 eV, respectively. That means, after gas adsorptions, the energy gaps of all the TM–doped BNNTs are lower than that of the pristine BNNT. These results indicate that electronic properties of TM–doped BNNTs are significantly changed by gas adsorptions. This reveals that the sensitivity of BNNT–based gas sensor for O_2 and PH_3 could be improved by introducing appropriate doping.

Natural bond orbital (NBO) analysis has been done to understand the charge transfer and orbital interactions established. The partial charge transfer was defined as $Q_{gas/BNNT} - Q_{gas}$, where $Q_{gas/BNNT}$ was the total charge of gas adsorbed on pristine or TM–doped BNNT and Q_{gas} was the total charge of O_2 or PH_3 in free case. The PCTs between O_2 and PH_3 molecules with pristine BNNT are –0.098 and 0.019 *e*, respectively. The small PCT values occurred during gas adsorption on pristine BNNT confirms a weak interaction between the BNNT and O_2 or PH_3 molecule. The PCTs between the O_2 and the TM–doped BNNTs are found in the range of –0.586 to –0.219 *e*, the PCT analysis indicates that partial charges transfer from TM–doped BNNTs to the O_2 molecule. The PCTs between the PH_3 and the TM–doped BNNTs are found in the range of 0.207 to 0.544 *e*, the PCT analysis indicates that partial charges transfer from the PH_3 to TM–doped BNNTs. In addition the PCTs of gas adsorption on TM–doped BNNTs are found to be larger than that of the pristine BNNT. This supports that the TM doping affects in the electronic properties of the bare BNNT after adsorptions

.

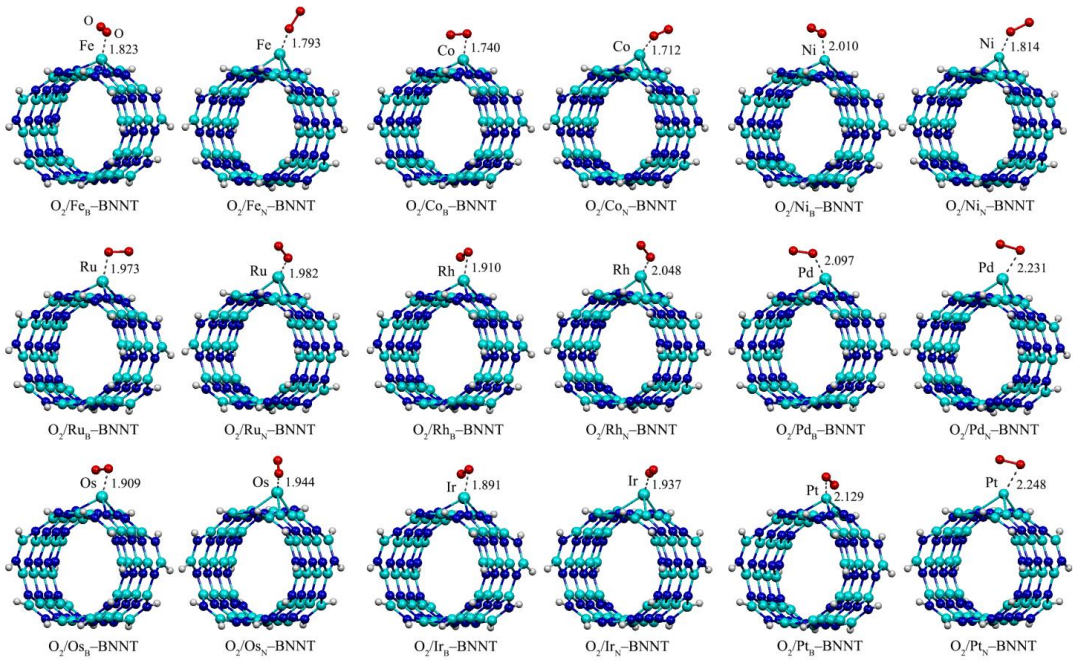

Figure 2 The optimized structures of O_2 adsorption on Fe_B–, Ru_B–, Os_B–, Co_B–, Rh_B–, Ir_B–, Ni_B–, Pd_B–, Pt_B–, Fe_N–, Ru_N–, Os_N–, Co_N–, Rh_N–, Ir_N–, Ni_N–, Pd_N–, and Pt_N–BNNTs. The boron, nitrogen, oxygen, and hydrogen atoms are presented in cyan, blue, red, and white balls, respectively. The doping TM atom is represented in cyan blue ball.

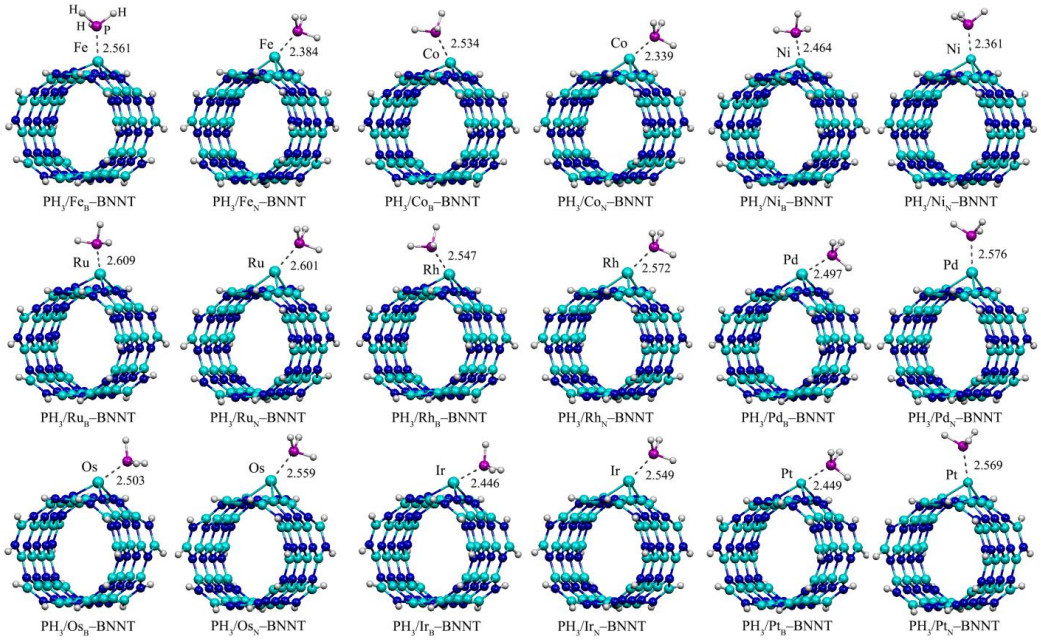

Figure 3 The optimized structures of PH_3 adsorption on Fe_B–, Ru_B–, Os_B–, Co_B–, Rh_B–, Ir_B–, Ni_B–, Pd_B–, Pt_B–, Fe_N–, Ru_N–, Os_N–, Co_N–, Rh_N–, Ir_N–, Ni_N–, Pd_N–, and Pt_N–BNNTs. The boron, nitrogen, phosphorus,

and hydrogen atoms are presented in cyan, blue, pink, and white balls, respectively. The doping TM atom is represented in cyan blue ball.

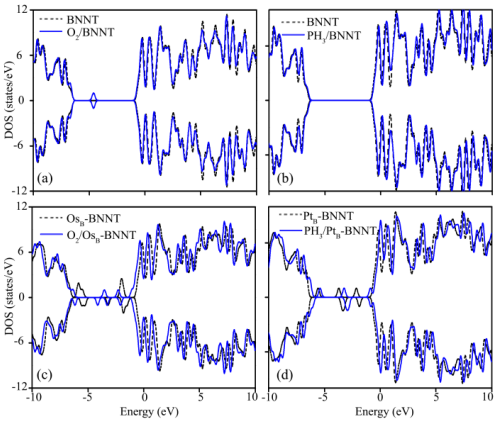

Figure 4 DOSs of pristine BNNT and their adsorptions with (a) O_2 and (b) PH_3 molecules and DOSs of (c) Os_B–BNNT and (d) Pt_B–BNNT and their gas adsorptions.

In order to further understand the electronic properties of the system, the DOSs of O_2 and PH_3 adsorbed on pristine and TM–doped BNNTs were computed and plotted (Figure 4). It is found that there is one DOS peak for both spin–up and spin–down electrons appearing at the Fermi lever. The DOS of pristine BNNT is insignificantly changed by gas adsorption which is in symmetry distribution between spin–up and spin–down channels, indicating that gas molecules had slightly sensible effect on the electronic properties of the tube (Figures 4a and 4b). However, the DOSs of the Os_B–BNNT (Figure 4c) and Pt_B–BNNT (Figure 4d) are changed by gas adsorptions, which are in asymmetry distribution between spin–up and spin–down channels. The DOS changes are expected to bring about obvious changes in the corresponding electronic properties. Accordingly, the TM–doped BNNTs are more suitable for sensing application for O_2 and PH_3 molecules.

4. Conclusions

The adsorption abilities of O_2 and PH_3 adsorbed on the pristine and Fe–, Ru–, Os–, Co–, Rh–, Ir–, Ni–, Pd–, and Pt–doped BNNTs at B or N sites were calculated. The TM–doped BNNTs display higher adsorption strength to O_2 and PH_3 molecules than the pristine BNNT. The O_2 molecule displays the highest adsorption interaction on Os_B–BNNT while the PH_3 molecule displays the highest adsorption interaction on Pt_B–BNNT. A significant increase in adsorption energy and charge transfer is probable to induce significant changes in the electrical conductivity of the TM–doped BNNTs. These calculations disclose that the TM–doped BNNTs can be used as O_2 and PH_3 storage and sensing in manufacturing raw materials.

5. Acknowledgements

The facilities provided by the Supramolecular Chemistry Research Unit and Department of Chemistry, Faculty of Science, Mahasarakham University are acknowledged. Financial support from the Center of Excellence for Innovation in Chemistry (PERCH–CIC) is also gratefully acknowledged.

6. References

[1] Chopra N.G., Luyken R.J., Cherrey K., Crespi V.H., Cohen M.L., Louie S.G. and Zettl A. Boron nitride nanotubes. *Science*. 1995. 269 : 966–967.

[2] Zhi C., Bando Y., Tang C. and Golberg D. Boron nitride nanotubes. *Mater. Sci. Eng. R Reports*. 2010. 70(3–6) : 92–111.

[3] Kalay S., Yilmaz Z., Sen O., Emanet M., Kazanc E. and Çulha M. Synthesis of boron nitride nanotubes and their applications. *Beilstein J. Nanotechnol*. 2015. 6(1) : 84–102.

[4] Xie Y., Huo Y.P. and Zhang J.M. First–principles study of CO and NO adsorption on transition metals doped (8, 0) boron nitride nanotube. *Appl. Surf. Sci*. 2012. 258 : 6391–6397.

[5] Tontapha S., Ruangpornvisuti V. and Wanno B. Density functional investigation of CO adsorption on Ni–doped single–walled armchair (5,5) boron nitride nanotubes. *J. Mol. Model.* 2013. 19 : 239–345.

[6] Al–Sunaidi A. Adsorption of SO_2 and NO_2 on metal–doped boron nitride nanotubes: A computational study. *Comput. Theor. Chem.* 2016. 1092 : 108–113.

[7] Chen Y., Hu C.L., Li J.Q., Jia G.X. and Zhang Y.F. Theoretical study of O_2 adsorption and reactivity on single–walled boron nitride nanotubes. *Chem. Phys. Lett.* 2007. 449 : 149–154.

[8] Liu H. and Turner C.H. Oxygen adsorption characteristics on hybrid carbon and boron nitride nanotubes. *J. Comput. Chem.* 2014. 35 : 1058–1063.

[9] Odling W. *A course of practical chemistry arranged for the use of medical students*. Longmans, Green, and Co., London, England, 1865.

[10] Gokhale S.D. and Jolly W. L. Phosphine, Inorg. Synth. 1967. 9 : 56–58.

[11] Gassmann G., Beusekom van J.E.E. and Glindemann D. Offshore atmospheric phosphine. *Naturwissenschaften.* 1996. 83(3) : 129–131.

[12] Srivastava P., Jaiswal N.K. and Sharma V. First–principles investigation of armchair boron nitride nanoribbons for sensing PH_3 gas molecules. *Superlattice Microst.* 2014. 73 : 350–358.

[13] Khan M.S., Srivastava A., Chaurasiya R., Khan M.S. and Dua P. NH_3 and PH_3 adsorption through single walled ZnS nanotube: First principle insight. *Chem. Phys. Lett*. 2015. 636 : 103–109.

[14] Frisch M.J., Trucks G.W., Schlegel H.B., Scuseria G.E., Robb M.A., Cheeseman J.R., Montgomery J.A., Vreven T., Kudin K.N., Burant J.C., Millam J.M., Lyengar S. S., Tomasi J., Barone V., Mennucci B., Cossi M., Scalmani G., Rega N., Petersson G.A., Nakatsuji H., Hada M., Ehara M., Toyota

K., Fukuda R., Hasegawa J., Ishida M., Nakajima T., Honda Y., Kitao O., Nakai H., Klene M., Li X., Knox J.E., Hratchian H.P., Cross J. B., Adamo C., Jaramillo J., Gomperts R., Stratmann R.E., Yazyev O., Austin A., Cammi R., Pomell C., Ochterski J. W., Ayala P.Y., Morokuma K., Voth G.A., Salvador P., Dannenberg J.J., Zakrzewski V G., Dapprich S., Daniels A. D., Strain M.C., Farkas O., Malick D.K., Rabuck A.D., Raghavachari K., Foresman J.B., Ortiz J., Cui Q., Baboul A.G., Clifford S., Cioslowski J., Stefanov B.B., Liu G., Liashenko A., Piskorz P., Komaromi I., Martin R.L., Fox D.J., Keith T., Laham M.A., Peng C.Y., Nanayakkara A., Challacombe M., Gill P.M., Johnson B., Chen W., Wong M.W., Gonzalez C. and Pople J.A. GAUSSIAN 09. Revision A.02, Gaussian Inc., Wallingford, CT, 2009.

[15] Lee C. , Yang W. and Parr R. G. Development of the Colle– Salvetti correlation– energy formula into a functional of the electron density. *Phys. Rev. B*. 1988. 37 : 785–789.

[16] Becke A.D. Density–functional thermochemistry. III The role of exact exchange. *J. Chem. Phys.* 1993. 98 : 5648–5652.

[17] Becke A.D. Density–functional exchange–energy approximation with correct asymptotic behavior. *Phys. Rev. A.* 1988. 38 : 3098–3100. Hay P.J. and Wadt W.R. *Ab initio* effective core potentials for molecular calculations. Potentials for the transition metal atoms Sc to Hg. *J. Chem. Phys.* 1985. 82 : 270–283.

[18] Hay P.J. and Wadt W.R. *Ab initio* effective core potentials for molecular calculations. Potentials for main group elements Na to Bi *J. Chem. Phys.* 1985. 82 : 284–298.

[19] Hay P.J. and Wadt W.R. Initio effective core potentials for molecular calculations. Potentials for K to Au including the outermost core orbital. *J. Chem. Phys.* 1985. 82 : 299–310.

[20] Buasaeng P., Rakrai W., Wanno B. and Tabtimsai C. DFT investigation of NH_3, PH_3, and AsH_3 adsorptions on Sc–, Ti–, V–, and Cr–doped single–walled carbon nanotubes. *Appl. Surf. Sci.* 2017. 400 : 506–514.

[21] Tabtimsai C., Nonsri A., Gratoo N., Massiri N., Suvanvapee P. and Wanno B. Carbon monoxide adsorption on carbon atom doped perfect and Stone–Wales defect single–walled boron nitride nanotubes: A DFT investigation. *Monatsh. Chem*. 2014. 145 : 725–735.

[22] Chandiramouli R., Srivastava A. and Nagarajan V. NO adsorption studies on silicene nanosheet: DFT investigation. 2015. *Appl. Surf. Sci*. 351 : 662–672.

[23] Liang W., Jia J., Lv J. and Wu H. Electronic structure, stability and magnetic properties of small $M_{1-2}Cr$ (M = Fe, Co, and Ni) alloy

encapsulated inside a $(BN)_{48}$ cage. *Phys. Lett. A*. 2015. 379 : 1715–1721.

[24] Yoosefian M., Zahedi M., Mola A. and Naserian S. A DFT comparative study of single and double SO_2 adsorption on Pt–doped and Au–doped single–walled carbon nanotube, *Appl. Sur. Sci.* 2015. 349 : 864–869.

[25] Tabtimsai C., Ruangpornvisuti V., Tontapha S. and Wanno B. A DFT investigation on group 8B transition metal–doped silicon carbide nanotubes for hydrogen storage application. *Appl. Surf. Sci.* 2018. 439 : 494–505.

[26] Flükiger P., Lüthi H.P. and Portmann S. MOLEKEL 4.3. Swiss Center for Scientific Computing, Manno, Switzerland, 2000.

[27] O'Boyle N.M., Tenderholt A.L. and Langner K.M. A library for package–independent computational chemistry algorithms. *J. Comput. Chem.* 2008. 29 : 839–845.

[28] Clementi E., Raimond D.L. and Reinhardt W.P. Atomic screening constants from SCF functions. II. Atoms with 37 to 86 Electrons. *J. Chem. Phys.* 1967. 47 (4) : 1300–1307.

[29] Linus P. Maximum–valence radii of transition metals. *Proc. Nat. Acad. Sci.* 1975. 72 : 3799–3801.

[30] Arenal R., Ferrari A.C., Reich S., Wirtz L., Mevellec J.Y., Lefrant S., Rubio A. and Loiseau A. Raman spectroscopy of single–wall boron nitride nanotubes. *Nano. Lett.* 2006. 6 : 1812–1816.